J Therm Anal Calorim (2012) 107:1321–1329
DOI 10.1007/s10973-011-1592-8

Experimental study of the influence of solvent and asphaltenes on liquid–solid phase behavior of paraffinic model systems by using DSC and FT-IR techniques

Luis Alberto Alcazar-Vara · Eduardo Buenrostro-Gonzalez

Received: 2 March 2011 / Accepted: 14 April 2011 / Published online: 1 May 2011

Abstract This experimental work presents the results of a study about the liquid–solid phase behavior of high molecular weight *n*-paraffins (C_{24}–C_{28} mixture and C_{36} pure) in aliphatic (*n*-decane and squalane) and aromatic (xylene and 1-phenyl dodecane) solvents. The effect of asphaltenes of different chemical nature over the liquid–solid behavior of heavy *n*-paraffins is also studied. Differential Scanning Calorimetry (DSC) was used to obtain the phase transitions onsets and enthalpies as well as the wax solubility curves. Crystallinity was studied by using both DSC and Infrared Spectroscopy (FT-IR) techniques. The results obtained and presented in this study showed that both, solvent and asphaltenes as well as their chemical nature have a significant effect on paraffin crystallization process.

Keywords Liquid–solid equilibrium · Wax precipitation · Solvent–solute interactions · Asphaltenes · Crystallinity

Introduction

Precipitation and deposition of high molecular weight *n*-paraffins (*wax*) and asphaltenes during the production, transportation, and processing of petroleum fluids is a common problem faced by the oil industry throughout the world. As the search for oil and gas moves toward deeper waters such as the Gulf of Mexico, the avoidance or remediation of wax deposition has become a key aspect of flow assurance [1]. Paraffin waxes in a crude oil start to precipitate when the surrounding temperature is lower than the wax appearance temperature (WAT) and they crystallize out of the solution to build a 3D network with a complex morphology [2]. It is generally regarded that waxes consist of branched (iso), cyclic and straight chain (normal) alkanes having chain lengths in excess of 17 carbon atoms (C_{17}) and potentially up to and over C_{100} [3]. However, it is generally accepted that the crystallizing materials that form the deposits are primarily *n*-alkanes [4, 5]. A description of the wax formation phenomenon involves both the study of the temperature of appearance of the first paraffinic crystals (WAT) and the determination of the amount of precipitated paraffins below WAT also called wax solubility or precipitation curves [6–8]. Gelation occurs when paraffin crystals interact to form volume-spanning networks which entrain the remaining liquid oil and impart solid-like mechanical properties to the fluid [9]. The key driving force behind deposition and gelling is the thermodynamic equilibrium of the solubility of the wax in the petroleum. Therefore, a better knowledge of factors affecting wax solubility will also improve the understanding of wax deposition problems in the petroleum industry [10]. The paraffin crystallization process can be influenced by many factors such as paraffin composition, solvent nature, polydispersity, rate of cooling, pressure, and the presence of impurities [10–15].

The studies about the effect of solvent on solubility of waxes reported in literature [10] have shown that waxes do not exhibit ideal solution behavior when crystallizing and that their solubility in a solvent increases as both the

L. A. Alcazar-Vara
Instituto Mexicano del Petróleo, Programa Académico de Posgrado, Eje Central Lázaro Cárdenas 152, 07730 Mexico, DF, Mexico
e-mail: laalcaza@imp.mx

E. Buenrostro-Gonzalez (✉)
Instituto Mexicano del Petróleo, Programa de Ingeniería Molecular, Eje Central Lázaro Cárdenas 152, 07730 Mexico, DF, Mexico
e-mail: ebuenro@imp.mx

solvent molecular size and solvent solubility parameter decrease. Furthermore, it has been reported that the miscibility of *n*-paraffins in solid state depends strongly on differences in molecular sizes (i.e., carbon number). An *n*-paraffin mixture with a significant carbon number difference (e.g., nC_{30}–nC_{36}) appears to form eutectic solids [16], whereas an *n*-paraffin mixture with a consecutive carbon number distribution forms a single orthorhombic solid solution [17].

The influence of the shape and size of the solvent on solute–solvent interaction and on the *n*-alkanes solubility has been also described in literature, hence it has been reported that globular or spherical solvents destroy the conformational order in liquid long-chain hydrocarbons [18, 19]. Aromatic solvents have been reported as a help in both inhibiting wax crystal formation and decreasing the amount of the wax deposited [20, 21].

In recent years, the effect of the presence of impurities such as asphaltenes on wax crystallization and gelation processes has been studied [15, 22–24]. The asphaltene fraction is formed by a variety of relatively large molecules containing aromatic rings, several heteroaromatic and naphthenic ring plus relatively short paraffinic branches [25]. Some authors have proposed that asphaltenes form aggregates with a core formed by aromatic regions, and aliphatic chains on the periphery interacting with the surrounding oil [26, 27] where these aliphatic portions promote interactions with waxes. In this way, some researchers have reported that asphaltenes play the role of nucleation sites for the wax crystallization, increasing or decreasing WAT [15, 23, 24] and affecting rheological properties [22, 24]. However, most of these experimental studies reported in literature have been carried out evaluating the effect of the solvent or asphaltenes on cloud point or wax dissolution temperatures. Nevertheless, the gelation and deposition processes are actually originated due to the amount of paraffin crystals formed during cooling below WAT. This makes important to evaluate the influence of solvent or asphaltenes on the amount of crystallized paraffin at temperatures below WAT.

The aim of this study is to get a better understanding of the crystallization mechanism of high molecular weight *n*-paraffins in the presence of solvents and asphaltenes of different chemical nature where the liquid–solid phase behavior and crystallinity are studied by means of Differential Scanning Calorimetry (DSC) and FT-IR spectroscopy.

Experimental section

Paraffinic model systems

The high molecular weight *n*-alkanes used in this study were obtained from Sigma-Aldrich with the following purity grades: tetracosane, $C_{24}H_{50}$ (99 wt%), octacosane, $C_{28}H_{58}$ (98 wt%), and hexatriacontane, $C_{36}H_{72}$ (98 wt%). Solvents used were also obtained from Sigma-Aldrich with the following purity grades: *n*-decane (99 wt%), 1-phenyldodecane, $C_{18}H_{30}$ (97 wt%), squalane, $C_{30}H_{62}$ (99 wt%), and xylene (97 wt%). The asphaltene samples used in this study, labeled as AsphPC and AsphIri, were extracted from two Mexican crude oils of the southern region. These asphaltenes of different chemical nature were characterized by using elemental analysis, vapor pressure osmometry, and ^{1}H and ^{13}C NMR spectroscopy to get their molecular parameters. A previous study with details of the experimental techniques used for the characterization of the asphaltenes and their effect on phase-equilibrium and rheological properties of waxy model systems has been submitted for publication. Table 1 shows some of the molecular parameters of the asphaltenes used in this study. As can be seen, the AsphPC asphaltenes are more aromatic than AsphIri asphaltenes, and its aromatic core is also bigger and more condensed, whereas the aromatic core of AsphIri asphaltenes is richer in alkyl substituents comprising methyl groups, alkyl chains, and naphthenic rings.

DSC

The DSC method has been widely used for the study of wax crystallization process [4, 12, 28] with satisfactory results due to its simplicity, accuracy, and fast response. The WAT, wax precipitation curves, crystallization, and melting properties were determined by using a Shimadzu DSC-60A differential scanning calorimeter. A calibration procedure was performed using an indium standard. The apparatus was continually flushed with nitrogen. Each sample (between 10 and 20 mg) was first heated, held isothermally for 1 min., and then cooled at a pre-defined rate of 5 °C/min. In order to delete any thermal history effects, two heating/cooling cycles were employed, so that crystallization and melting properties were obtained from the second cycle. The onset crystallization temperature (WAT) was determined as the onset of the exothermic peak during the cooling process corresponding to the liquid–solid transition. Under heating conditions, the melting temperature was recorded as the onset of the endothermic peak, whereas the wax disappearance temperature (WDT), temperature at which the last precipitated paraffin re-dissolves in the solvent, was recorded as the temperature of the endothermic peak. The total energy released during cooling or heating process is proportional to the area between the base line and the exothermic peak or endothermic peak, respectively, so that the enthalpies of crystallization and melting were calculated from the integration of heat flow curve. Assuming that the amount or fraction of precipitated wax in the total wax content is proportional to

Table 1 Molecular parameters of AsphPC and AsphIri asphaltenes

Symbol	Definition	Asphaltene sample	
		AsphIri	AsphPC
R_A	Aromatic rings	7.09	20.69
f_a	Aromaticity factor	0.50	0.67
ϕ	Condensation index	0.53	0.71
n	Average number of carbon atoms per alkyl substituents	5.99	5.47
σ	Aromatic substitution index	0.55	0.37
n_{ac}	Average length of the alkyl chains	11.84	11.12

the percent of accumulated heat released in the total heat released (crystallization enthalpy), the amount of precipitated wax at different temperatures can be determined by dividing the accumulated heat released by the heat of crystallization as has been reported in literature [7, 8, 29, 30]. The method described for the determination of the wax precipitation curve is depicted in Fig. 1, where the accumulated heat released for the exothermic peak related to the crystallization of the system 6 wt% of C_{36} in *n*-decane is plotted as an example.

The degree of crystallinity for pure solutes in solvent systems was calculated by the following equation [31]:

$$\text{Percent crystallinity} = \frac{\Delta H_m}{\Delta H_{m^\circ}} \times 100, \quad (1)$$

where ΔH_m is the melting enthalpy of model system measured by DSC and ΔH_{m° is the melting enthalpy of the 100% crystalline solute.

Infrared spectroscopy (FT-IR)

The FT-IR was used to study in a qualitative way the effect of asphaltenes over the crystallinity of solid phase formed below the WAT for the C_{24}–C_{28} paraffinic model system. The FT-IR spectra were obtained by using a Bruker Tensor 27 spectrometer along with Opus v6.5 software. The FT-IR spectra were collected in the range of 4000–600 cm^{-1}. The spectra obtained were an average of 16 scans with a spectral resolution of 4.0 cm^{-1}. The sample placed between NaCl windows (41 × 23 × 6 mm, 0.1 mm lead spacer) was loaded in a reflex liquid cell fitted into the heating/cryogenic jacket. The sample temperature was measured with a calibrated type-K thermocouple inserted into the thermocouple well of the sample cell holder by using a Fluke 51 II digital thermometer. The temperature was controlled by using a Neslab RTE-101 bath circulator. The experiments were carried out at a cooling rate of 1 °C/min.

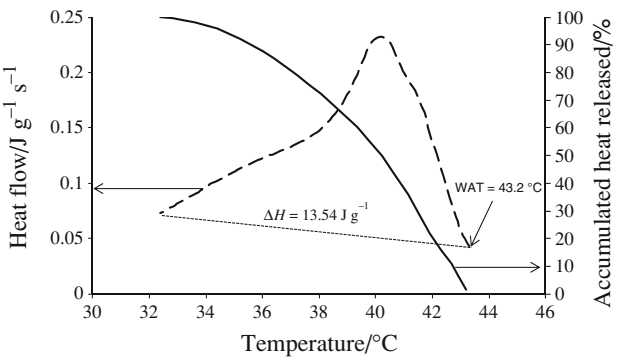

Fig. 1 Accumulated heat released for the DSC exothermic peak used for determination of wax precipitation curve of the system 6 wt% of C_{36} in *n*-decane

Results and discussion

Effect of chemistry solvent on liquid–solid phase behavior

Figure 2 shows the DSC thermograms of the crystallization and melting behavior of 6 wt% of hexatriacontane (C_{36}) in different pure and mixed solvents systems. As can be seen, a single and well-defined peak is observed during cooling and heating processes, related to the crystallization and melting of the monodisperse sample of the heavy paraffin C_{36} in different solvent systems. However, the endothermic peaks seem to be broader than the exothermic, so while the identification of the crystallization onset temperatures was straightforward; the melting onset temperatures were difficult to identify.

Crystallization and melting properties of the model systems investigated are shown in Table 2. The influence of the solvent aromaticity over the solution of C_{36} in *n*-decane was studied by adding mono-aromatic solvents: xylene and 1-phenyldodecane. The data show clearly the effect of the solvent chemistry on those properties. Lower values of crystallization and melting enthalpies are obtained in the presence of aromatic solvents. The magnitude of the enthalpies decreasing is related to the aromaticity of the solvent mixture, where greater aromaticity causes a greater diminishing of crystallization and melting enthalpies. Hence, the aromatic single rings interspersed

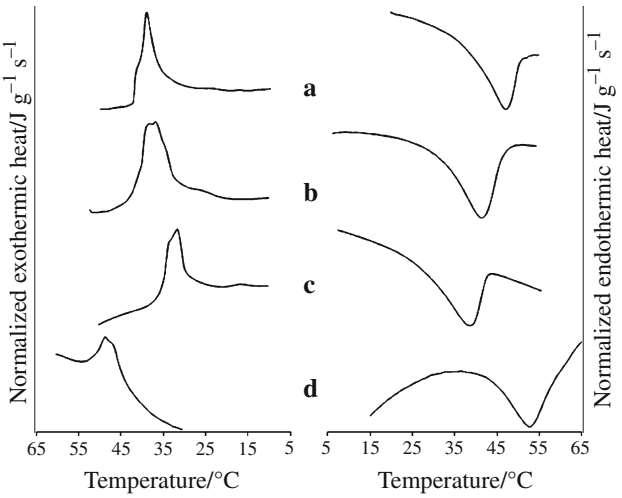

Fig. 2 DSC exothermic and endothermic peaks of 6 wt% of C_{36} in different simple and mixed solvents systems: (*a*) 94% of *n*-decane, (*b*) 47% *n*-decane + 47% 1-phenyldodecane, (*c*) 47% *n*-decane + 47% xylene, and (*d*) 94% of squalane

among hexatriacontane molecules hinder their interactions, preventing an efficient ordering during cooling, then the paraffin crystal networks of a solid phase formed in such circumstance result significantly less ordered, as indicated by the lower values of the crystallinity index calculated from DSC data (see Table 3) for the model systems with aromatic solvents.

A way to explain the depressing effect of aromatic solvents over the enthalpies of crystallization and melting is through the entropy change that suffers the system during liquid–solid phase transition. It can be assumed that magnitude of the entropy change in the crystallization and melting processes for a paraffinic–aromatic mixture is lower than that for a 100% aliphatic system, like the C_{36}-*n*-decane system, because of the poor crystal network ordering of the solid phase formed in the presence of aromatic solvents, which is reflected in the lower values of their crystallinity index. For another hand, a crystal network with greater disorder introduced by the aromatic molecules of the solvent is weaker, so its melting temperature tends to be lower. The WAT is also lowered due to the presence of aromatic solvents; however, in the case of the 1-phenyldodecane, a less aromatic solvent than xylene and with a greater molecular weight than decane, its aliphatic chain of 12 carbons has a significant "ordering" effect in the paraffinic crystal network that surpasses the effect of its aromatic rings regards to the depressing of the WAT and melting temperature observed with the xylene.

In contrast, by changing the solvent system from *n*-decane to squalane (a C_{24} aliphatic chain with six methyl branches), the WAT is significantly increased to 54.5 °C with a dramatic depression of the enthalpy of crystallization. This behavior is influenced by the size and structure of the solvent, in a similar way to that observed for the 1-phenyldodecane–*n*-decane solvent system. The methyl branches of the C_{24} iso-paraffin inhibits the efficient ordering of C_{36} molecules during crystallization process, forming a less ordered solid phase than that formed in C_{36}-decane system, which is reflected in the low enthalpy of crystallization measured (6.36 J/g); on the other hand, the highest WAT observed is a consequence of the greater size of squalane respect to decane. In fact, as has been reported, solubility decreases (greater WAT) as the solvent size increases due to the inability of the bigger solvent molecule to effectively contact and solvate the solute [10]. Furthermore, despite the disorder in the crystalline arrangement caused by the six methyl branches of the squalane, the effect of its size (24 carbon length) results in the highest values of both temperature and enthalpy of melting.

Table 2 shows also the WDT of C_{36} in different solvents during melting process. Under ideal conditions, the values of WAT and WDT should be similar; however, as has been reported [4], differences between both values can be attributed to the experimental uncertainty and kinetic effects (e.g., supercooling). Our DSC results showed differences in the range between 0.88 and 5.38 °C which could be attributed to the heating/cooling rate used of 5 °C/min. The effect of solvent chemistry on WDT of C_{36} was similar to that observed for the melting temperature discussed above.

The results presented before showed a significant influence of solvent chemistry on crystallization and

Table 2 Crystallization and melting properties of the system 6% of C_{36} in different solvents systems

Solvent system	WAT/°C	Enthalpy of crystallization/J g^{-1}	Melting temperature/°C	Enthalpy of melting/J g^{-1}	WDT/°C	Aromaticity of the solvent system[a]
94% *n*-decane	43.2	13.54	30.52	12.48	45.6	0
47% *n*-decane + 47% xylene	37.5	8.05	11.96	9.31	37.92	0.43
47% *n*-decane + 47% 1-phenyldodecane	47.5	10.66	20.25	10.09	41.82	0.12
94% Squalane	54.5	6.36	37.1	12.56	52.89	0

[a] Calculated as the aromaticity factor of aromatic solvent multiplied by its molar fraction in the mixture, where aromaticity factor of the xylene and 1-phenyldodecane are 0.75 and 0.333, respectively

Table 3 DSC crystallization data of the system 6% of C_{36} in different solvent systems

Solvent system	Onset crystallization temperature/°C	Endset crystallization temperature/°C	ΔT/°C[a]	Δt/min[b]	DSC crystallinity/%[c]
94% *n*-decane	43.2	32.4	10.8	2.16	7.21
47% *n*-decane + 47% xylene	37.5	23.5	14	2.8	5.38
47% *n*-decane + 47% 1-phenyldodecane	47.5	22.5	25	5	5.83
94% Squalane	54.5	41.08	13.42	2.68	7.26

[a] ΔT = Onset–Endset

[b] For a cooling rate = 5 °C/min

[c] For a melting enthalpy of hexatriacontane = 172.9 J/g [32]

melting of C_{36}; however, to get a better understanding of the paraffin crystallization process in the presence of solvents of different chemical structure at temperatures below WAT, solubility curves were obtained by using the DSC data as can be seen in Fig. 3. As expected, the crystallization process of C_{36} in squalane starts before respect to the other systems, as a consequence of solvent chain length, followed by the other mixtures according with their respective WATs.

The chemical structure of the solvent affects significantly the crystallization rate of the hexatriacontane C_{36}. Table 3 shows that the crystallization process is slower for the systems with aromatic solvents. An evident consequence of this is the fact that lower amounts of solids are formed in these systems respect to the decane system below of its WAT as can be observed in Fig. 3, this can be attributed to the aromatic ring interfering with the normal crystal growth, retarding the conformational ordering of C_{36} molecules in the solid phase created.

The degree of crystallinity obtained by DSC for the solid phase formed in the presence of squalane, shown in Table 3, points out the effect of competition between the size and branching of the aliphatic solvents in the crystallinity of the solid phases formed. Due to the greater size of squalane regard to the *n*-decane, it would be expected a greater crystallinity index for the solid phase formed in the presence of squalane; however, its ramifications limit the possibility of achieving an efficient conformational ordering of the crystal network in the solid phase, which results in a crystallinity index value similar to that obtained for the *n*-decane system.

Effect of asphaltenes on liquid–solid phase behavior

The effect of solvent and asphaltenes was studied on liquid–solid equilibrium of the binary system C_{24}–C_{28}. The composition used in these model systems was 15 and 10 wt% of C_{24} and C_{28}, respectively, in the following solvent systems: (a) 75% of decane, (b) mixture of 37.5% of decane + 37.5% of xylene, and (c) mixture of 37.5% of decane + 37.0% of xylene + 0.5% of asphaltenes. DSC exothermic peaks of these model systems are plotted in Fig. 4 and their crystallization properties are shown in Table 4. As can be seen, the presence of an aromatic solvent as the xylene decreases slightly both WAT and crystallization enthalpy due to the disorder effects generated by

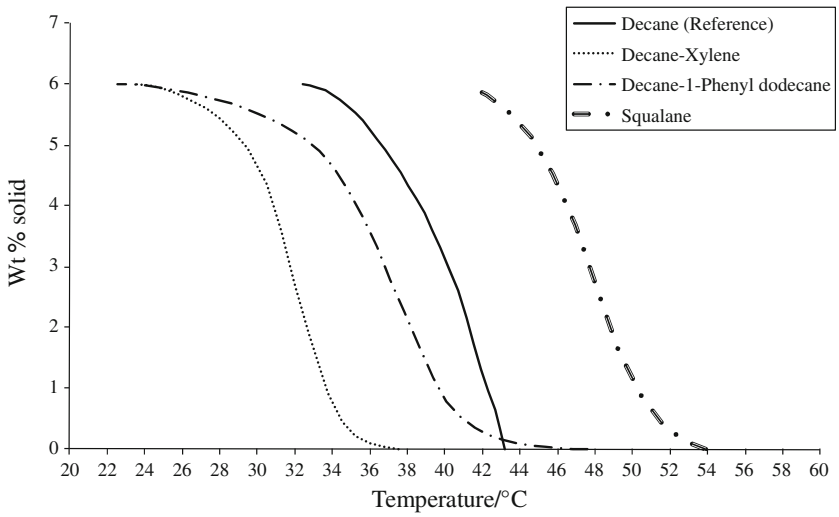

Fig. 3 DSC solubility curves of 6 wt% of C_{36} in different simple and mixed solvents systems

the aromaticity as was discussed before. However, crystallization properties were notably affected by the presence of asphaltenes where their chemical nature played an important role. It has been reported that flocculated asphaltenes providing nucleation sites for waxes increase WAT [15, 23], but also it has been reported [24] that asphaltenes decreased very slightly the WAT, according to this last study the effect of the asphaltenes on the WAT depends of the aggregation state of the asphaltenes.

In our model systems, the results obtained showed a slight increasing of WAT due to the presence of the aliphatic asphaltenes (AsphIri) and a decrease in the presence of the more aromatic asphaltenes (AsphPC) with respect to the C_{24}–C_{28} in decane–xylene model system without asphaltenes. For another hand, the crystallization heat increases significantly in the presence of AsphIri asphaltenes, whereas diminishes moderately in the presence of AsphPC asphaltenes. These results make evident the effect of the chemical nature of different asphaltenes over the crystallization behavior of paraffinic systems. A greater abundance of aliphatic chains in AsphIri asphaltenes permits a better interaction with the paraffins of the C_{24}–C_{28} system promoting co-crystallization phenomena, where the asphaltenes are partially integrated to the crystal network and probably acting as nucleation sites, causing a slight increasing of WAT. Moreover, the partial immobilization of the paraffins engaged in the interactions with the asphaltene alkyl chains may promote a "*quasicrystallization*" phenomenon of the paraffins in the asphaltene network, such interaction results in exothermic effects as has been reported in literature [33, 34], which explains the significant increase of crystallization heat of the model system with AsphIri asphaltenes as is observed in Table 4. On the other hand, the most aromatic asphaltenes (AsphPC) with a bigger and more condensed aromatic core and with a smaller amount of aliphatic substituents inhibit in some extent the paraffin–asphaltene interactions so that they cannot be incorporated to the paraffin crystal structure hindering nucleation process and crystal network growth, which results in a WAT decrease with a lower crystallization enthalpy due to the formation of a disordered solid phase.

The wax solubility curves of these systems are plotted in Fig. 5, as can be seen the effect of solvent and asphaltenes of different chemical nature is evident. Regarding to the C_{24}–C_{28} mixture in *n*-decane, the presence of xylene reduces moderately both the amount of solid formed and the WAT, although the temperature interval of their solubility curves are very similar. However, the effect of asphaltenes on wax solubility curve is very significant considering its low concentration in the model system (0.5%), particularly in the case of the more aromatic AsphPC asphaltene. As in the case of C_{36} in different solvents, the rate of wax precipitation for the C_{24}–C_{28} mixture in xylene is significantly affected by the presence of a small amount of highly aromatic compounds such as the asphaltenes. The data in Table 4 shows also that the presence of asphaltenes in the paraffinic system increases around 25% the time required to precipitate the total of paraffins (Δt) for a cooling rate of 5 °C/min.

These results show that asphaltenes are practically acting in this system as inhibitors of the paraffins precipitation. When the asphaltenes have a structure highly condensed with a certain degree of aromatic substitution, that allows some kind of interaction with the paraffins, the inhibition effect is greater due to the steric interference and the disorder generated in the paraffinic network which difficult the molecular recognition among paraffin molecules avoiding the growth of stable crystalline networks and therefore the formation of the solid phase. Otherwise a less condensed aromatic structure with a greater substitution degree have a better interaction with paraffins and thus, it could play a role as nucleation site increasing both WAT and the amount of solid phase formed, at least in a certain temperature range as can be observed in Fig. 5, but even in such case the disruptive effect that introduces the

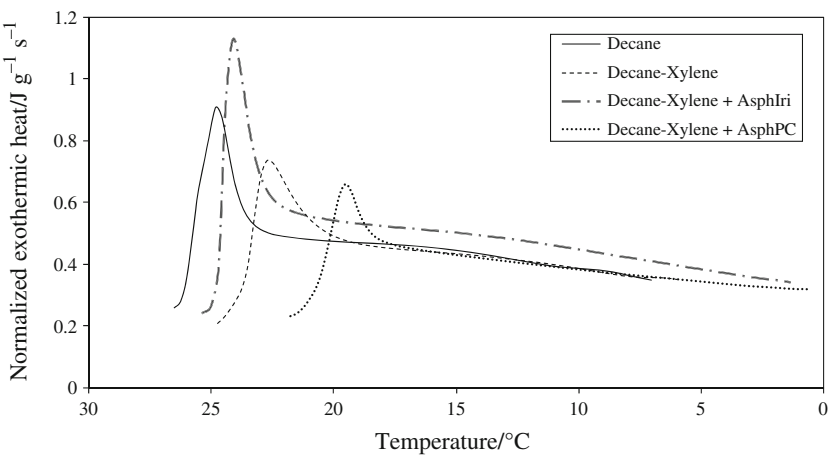

Fig. 4 DSC exothermic peaks of the binary system C_{24}–C_{28} in different solvent systems and with asphaltenes of different chemical nature

Table 4 DSC crystallization data of the binary system C_{24}–C_{28} in different solvent systems and with asphaltenes

Solvent system	WAT/°C	Enthalpy of crystallization/J g^{-1}	Endset/°C	ΔT/°C[a]	Δt/min[b]
Decane	26.5	37.09	7	19.5	3.9
Decane–xylene	24.81	36.51	6.09	18.72	3.74
Decane–xylene + AsphIri	25.66	58.42	1	24.66	4.93
Decane–xylene + AsphPC	21.77	33.01	0.53	21.24	4.24

[a] WAT-endset

[b] For a cooling rate = 5 °C/min

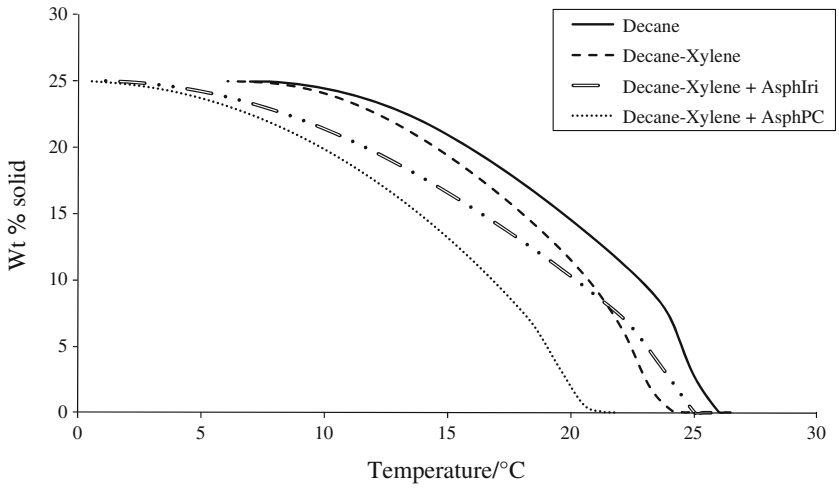

Fig. 5 Wax solubility curves of the binary system C_{24}–C_{28} in different solvent systems and with asphaltenes of different chemical nature

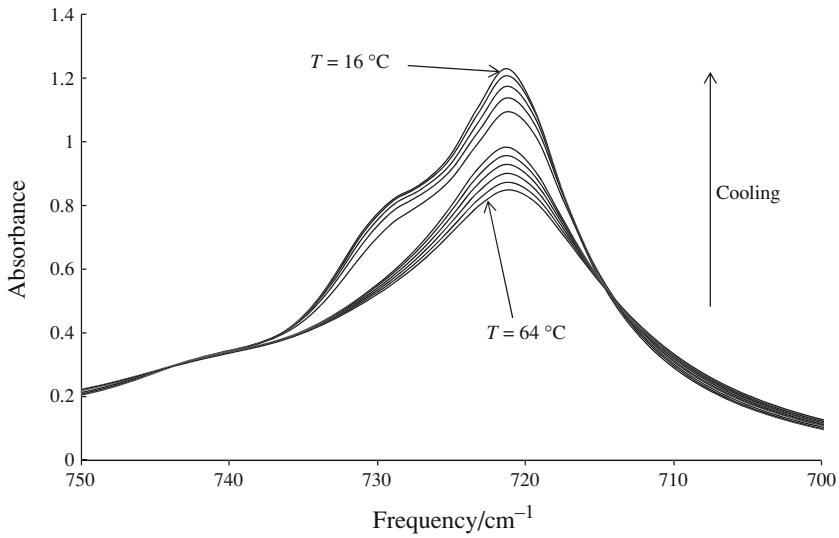

Fig. 6 Spectra at 720 cm^{-1} and at different temperatures of the system 6 wt% of hexatriacontane (C_{36}) in *n*-decane

aromatic core of the asphaltenes prevails inhibiting the crystallization process, as it was observed for the model system with the AsphIri asphaltenes.

The absorbance bands of the infrared spectrum in the region between the wave numbers 735 and 715 cm^{-1} have been attributed to the rocking vibrations of long chain methylene (LCM) groups that have four or more CH_2 segments [35]. The LCM group is a major component of the solid wax. The absorbance in this region increases as the temperature of the hydrocarbon sample decreases, due to the density change.

In Fig. 6 the FT-IR spectra at 720 cm^{-1} obtained at different temperatures during cooling of the system formed by 6 wt% of hexatriacontane (C_{36}) in *n*-decane are shown. At temperatures above WAT (43.2 °C), a single IR absorption peak is obtained at 721 cm^{-1} indicating the

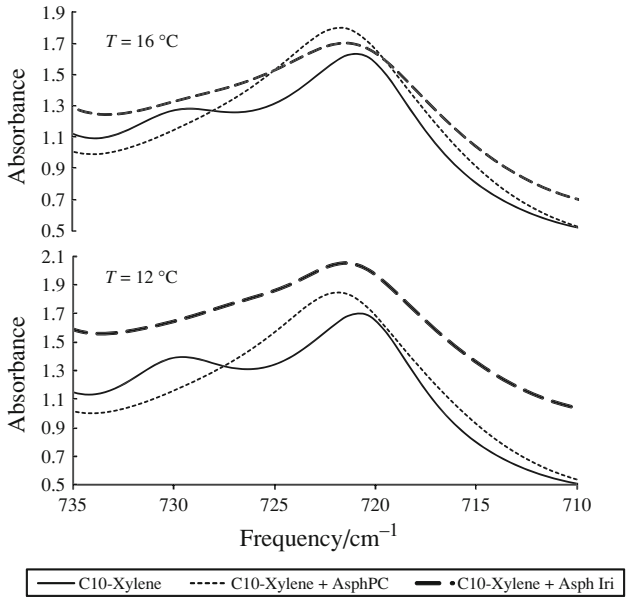

Fig. 7 Effect of asphaltenes on FT-IR spectra (735–715 cm^{-1}) at temperatures of 16 and 12 °C of the model system C_{24}–C_{28} in *n*-decane + xylene

conformationally disordered structure of an amorphous liquid phase. However, as the temperature is lowered an splitting of this peak into a doublet is developed at 730 and 721 cm^{-1}, which indicate the presence of an ordered crystalline (orthorhombic) phase (730 cm^{-1}) and a less disordered amorphous liquid phase at 721 cm^{-1} [6, 36, 37].

The FT-IR spectra obtained allowed qualitatively examining the effect of the asphaltenes on the crystallinity of the paraffinic solid phase. Figure 7 shows the FT-IR spectra in the range of 735–715 cm^{-1} of the system C_{24}–C_{28} in *n*-decane + xylene with and without asphaltenes at temperatures below the WAT, 16 and 12 °C. At 730 cm^{-1} the model system without asphaltenes shows the characteristic peak attributed to the creation of a crystalline (orthorhombic) phase, whereas in the model systems with asphaltenes this peak is not exhibited indicating a reduced crystallinity of the solid phase formed in the presence of these heavy aromatic compounds.

Conclusions

The liquid–solid phase equilibrium of the paraffinic model systems studied in this study was affected by the chemical nature of the solvent used. The aromaticity was found to be a key factor that results in inhibition of the paraffin crystallization process, decreasing WAT, by promoting the creation of a solid phase partially disordered due to the presence of aromatic single rings interspersed among paraffin molecules hindering their efficient ordering during cooling. On the other hand, the presence of asphaltenes in the model paraffinic systems, even at small concentrations, has a significant influence over the liquid–solid phase transition of such systems. The asphaltenes effect over the WAT and wax precipitation curve depends on their chemical nature. The asphaltene aliphatic chains promote a better asphaltene–wax interaction resulting in an easier incorporation of asphaltenes into the wax crystal network, where the normal crystal growth is just partially affected, whereas the aromatic core of the asphaltenes causes steric interference among paraffin molecules that inhibits and disturbs the wax crystal growth which results in both, retarding the crystallization process and decreasing the amount of precipitated paraffin at temperatures below WAT with a significant reduction of the crystallinity of the solid phase created.

According to the results presented in this study, the presence of a certain amount of asphaltenes in the crude oil could naturally reduce the severity of the problems associated with the formation of wax deposits in pipelines and hydrocarbon production facilities. Although asphaltenes under certain conditions may increase the wax formation temperature, the wax deposits formed in the presence of asphaltenes would tend to be unstable and weak, therefore much easier to remove or dissolve.

Acknowledgements The authors express gratitude to the Instituto Mexicano del Petróleo (IMP) for both providing facilities and granting permission to publish results. L.A.A.V thanks CONACYT and the Programa Académico de Posgrado of IMP for the economic support granted during his Ph.D studies.

References

1. Coutinho JAP, Edmonds B, Moorwood T, Szczepanski R, Zhang X. Reliable wax predictions for flow assurance. Energy Fuels. 2006;20:1081–8.
2. Venkatesan R, Nagarajan NR, Paso K, Yi YB, Sastry AM, Fogler HS. The strength of paraffin gels formed under static and flow conditions. Chem Eng Sci. 2005;60:3587–98.
3. Flow assurance design guideline. Deepstar IV project. 2001.
4. Hansen AB, Larsen E, Pedersen WB, Nielsen AB. Wax precipitation from North Sea crude oils. 3. Precipitation and dissolution of wax studied by differential scanning calorimetry. Energy Fuels. 1991;5:914–23.
5. Singh P, Fogler HS, Nagarajan N. Prediction of the wax content of the incipient wax–oil gel in a pipeline: an application of the controlled-stress rheometer. J Rheol. 1999;43:1437–59.
6. Roehner RM, Hanson FV. Determination of wax precipitation temperature and amount of precipitated solid wax versus temperature for crude oils using FT-IR spectroscopy. Energy Fuels. 2001;15:756–63.
7. Han S, Huang Z, Senra M, Hoffmann R, Fogler HS. Method to determine the wax solubility curve in crude oil from centrifugation and high temperature gas chromatography measurements. Energy Fuels. 2010;24:1753–61.
8. Coto B, Martos C, Peña JL, Espada JJ, Robustillo MD. A new method for the determination of wax precipitation from

non-diluted crude oils by fractional precipitation. Fuel. 2008; 87:2090–4.
9. Paso K, Senra M, Yi Y, Sastry AM, Fogler HS. Paraffin polydispersity facilitates mechanical gelation. Ind Eng Chem Res. 2005;44:7242–54.
10. Jennings DW, Weispfennig K. Experimental solubility data of various n-alkane waxes: Effects of alkane chain length, alkane odd versus even carbon number structures and solvent chemistry on solubility. Fluid Phase Equilib. 2005;227:27–35.
11. Garcia MD, Carbognani L, Orea M, Urbina A. The influence of alkane class-types on crude oil wax crystallization and inhibitors efficiency. J Petrol Sci Eng. 2000;25:99–105.
12. Senra M, Panacharoensawad E, Kraiwattanawong K, Singh P, Fogler HS. Role of *n*-alkane polydispersity on the crystallization of *n*-alkanes from solution. Energy Fuels. 2008;22:545–55.
13. Vieira LC, Buchuid MB, Lucas EF. Effect of pressure on the crystallization of crude oil waxes. II. Evaluation of crude oils and condensate. Energy Fuels. 2010;24:2213–20.
14. Guo X, Pethica BA, Huang JS, Adamson DH, Prud'homme RK. Effect of cooling rate on crystallization of model waxy oils with microcrystalline poly(ethylene butane). Energy Fuels. 2006;20: 250–6.
15. Garcia MC. Crude oil wax crystallization. The effect of heavy *n*-paraffins and flocculated asphaltenes. Energy Fuels. 2000;14: 1043–8.
16. Dorset DL, Snyder RG. Crystal structure of modulated *n*-paraffin binary solids. J Phys Chem. 1996;100:9848–53.
17. Dirand M, Chevallier V, Provost E, Bouroukba M, Petitjean D. Multicomponent paraffin waxes and petroleum solid deposits: structural and thermodynamic state. Fuel. 1998;77:1253–60.
18. Kniaz K. Influence of size and shape effects on the solubility of hydrocarbons: the role of the combinatorial entropy. Fluid Phase Equilib. 1991;68:35–46.
19. Domanska U, Morawski P. Influence of size and shape effects on the high-pressure solubility of *n*-alkanes: experimental data, correlation and prediction. J Chem Thermodyn. 2005;37: 1276–87.
20. Rakotosaona R, Bouroukba M, Petitjean D, Dirand M. Solubility of a petroleum wax with an aromatic hydrocarbon in a solvent. Energy Fuels. 2008;22:784–9.
21. Ray SS, Pandey NK, Chatterjee AK. Effect of aromatics and *iso*-alkanes on the pour point of different types of lube oils. Fuel. 2009;88:1629–33.
22. Venkatesan R, Ostlund JA, Chawla H, Wattana P, Nyden M, Fogler HS. The effect of asphaltenes on the gelation of waxy oils. Energy Fuels. 2003;17:1630–40.
23. Kriz P, Andersen SI. Effect of asphaltenes on crude oil wax crystallization. Energy Fuels. 2005;19:948–53.
24. Tinsley JF, Jahnke JP, Dettman HD, Prud'home RK. Waxy gels with asphaltenes 1: characterization of precipitation, gelation, yield stress, and morphology. Energy Fuels. 2009;23:2056–64.
25. Speight JG. The chemistry and technology of petroleum. 3rd ed. New York: Marcel-Dekker; 1999.
26. Mullins OC, Betancourt SS, Cribbs ME, Dubost FX, Creek JL, Andrews AB, Venkataramanan L. The colloidal structure of crude oil and the structure of oil reservoirs. Energy Fuels. 2007;21: 2785–94.
27. Carbognani L, Rogel E. Solid petroleum asphaltenes seem surrounded by alkyl layers. Petrol Sci Technol. 2003;21:537–56.
28. Guo X, Pethica BA, Huang JS, Prud'homme RK. Crystallization of long-chain *n*-paraffins from solutions and melts as observed by differential scanning calorimetry. Macromolecules. 2004;37: 5638–45.
29. Coutinho JAP, Calange S, Ruffier-Meray V. Measuring the amount of crystallinity in solutions using DSC. Can J Chem Eng. 1997;75:1075–9.
30. Coutinho JAP, Ruffier-Meray V. Experimental measurements and thermodynamic modeling of paraffinic wax formation in undercooled solutions. Ind Eng Chem Res. 1997;36:4977–83.
31. Conti DS, Yoshida MI, Pezzin SH, Coelho LAF. Miscibility and crystallinity of poly(3-hydroxybutyrate)/poly(3-hydroxybutyrate-co-3-hydroxyvalerate) blends. Thermochim Acta. 2006;450: 61–6.
32. Dirand M, Bouroukba M, Chevallier V, Petitjean D, Behar E, Ruffier-Meray V. Normal alkanes, multialkane synthetic model mixtures, and real petroleum waxes: crystallographic structures, thermodynamic properties and crystallization. J Chem Eng Data. 2002;47:115–43.
33. Mahmoud R, Gierycz P, Solimando R, Rogalski M. Calorimetric probing of *n*-alkane–petroleum asphaltene interactions. Energy Fuels. 2005;19:2474–9.
34. Stachowiak C, Viguie JR, Grolier JP, Rogalski M. Effect of *n*-alkanes on asphaltene structuring in petroleum oils. Langmuir. 2005;21:4824–9.
35. Smith B. Infrared spectral interpretation, a systematic approach. New York: CRC Press; 1999.
36. Hagemann H, Snyder RG, Peacock AJ, Mandelkern L. Quantitative infrared methods for the measurement of crystallinity and its temperature dependence: polyethylene. Macromolecules. 1989; 22:3600–6.
37. Yoshida H. Structure relaxation of *n*-alkanes observed by the simultaneous DSC–FTIR method. J Therm Anal Calorim. 1999; 57:679–85.